Indian Journal of Chemistry
Vol. 60A, September 2021, pp. 1151-1158

Molecularly imprinted electrochemical sensor based on electrode modified by functionalized carbon nanotube for selective detection of uric acid

Yongfu Zhao*, Hui Liu, Wen Lv & Yanhuan Wang

College of Chemistry and Chemical Engineering, Zhengzhou Normal University, Zhengzhou 450044, P R China

*E-mail: zhaoyongfu2008@163.com

Received 22 June 2021; revised and accepted 03 September 2021

In this study, we have developed a novel biomimetic electrochemical sensor sensitized with functionalized carbon nanotubes using a molecularly imprinted film as a recognition element for the rapid detection of uric acid. Using $K_3[Fe(CN)_6]$ as a probe, uric acid imprinted films on electrodes are characterized by voltammetry measurements and electrochemical impedance spectroscopy. The optimizations of experimental steps are conducted by cyclic voltammetry and differential pulse voltammetry. When the imprinted sensor is immersed in the solution containing a certain concentration of uric acid and incubated for a period of time, the oxidation peak current of $K_3[Fe(CN)_6]$ decreases with the increase of uric acid concentration. Under optimal conditions, the peak current of $K_3[Fe(CN)_6]$ has a good linear relationship with uric acid concentration at range from 0.1 μM to 3.3 μM with the detection limit of 0.03 μM. The proposed sensor shows high selectivity for rapid detection of uric acid in human serum samples.

Keywords: Molecular imprinting, Uric acid, Electropolymerization, Functionalized carbon nanotube, Electrochemical sensor

Uric acid (UA) is a final product of purine metabolism in human body and its concentration in normal adult human body is relatively stable. The normal level of UA in human blood serum is 0.12-0.45 mM and in urine is 1.49-4.46 mM[1,2]. Elevated levels of UA can cause cardiovascular disease, nephropathy, diabetes and other diseases. Therefore, monitoring of UA level in human blood and urine is very important for the prevention of the mentioned diseases. By now various techniques have been developed for UA detection, such as enzymatic assay[3,4], high-performance liquid chromatography[5,6], chemiluminescence[7,8], colorimetry[9-11]. However, these methods inherit some problems such as high cost, time-consuming, complex instruments, trained operators, which are not suitable for on-spot analysis. The electrochemical method for the determination of UA has attracted wide attention owing to its several advantages including rapid detection, low cost and high sensitivity[12-15]. However, the practical applications of electrochemical method is limited by the poor selectivity and reproducibility resulting from factor that UA is oxidized at a potential rather close to that of ascorbic acid, dopamine, which often coexist with UA in a biological fluid[1,16-18]. Therefore, the development of new electrochemical sensors to improve the sensitivity of UA detection remains of great significance for clinical diagnostics.

Molecular imprinting is a promising technique which offers template-assisted formation of selective recognition sites in a synthetic polymeric network capable of mimicking the biorecognition ability of biomolecules such as amino acids, nucleic acids, enzymes and antibodies etc.[19,20]. In this method, molecularly imprinted polymer (MIP) is "plastic antibody" which is synthesized by template molecule and functional monomer[21,22]. After the template molecule is removed from the polymeric network, binding sites complementary to the template in size, shape and orientation are created, which serve as a functional recognition element for sensing processes. Molecular imprinting technique has properties such as high stability, low cost, high sensitivity and selectivity, which enable the use of it for electrochemical sensing applications in a broad variety of areas such as biological analysis[23], pharmaceutical analysis[24], food safety[25] and environmental sciences[26]. Therefore, it is of great importance to develop electrochemical sensors based molecular imprinting technique for achievement of selective and efficient determination of target molecules.

However, the relatively low conductivity and electrocatalytic activity of MIPs reduce the sensitivity

of the electrochemical sensor[27]. Therefore, the electrodes are modified with conductive nanomaterials especially carbon-based materials and a thin MIP layer formed on the surface of the electrodes to increase the conductivity of the sensor[28-30]. Additionally, the electrochemical sensor combined with the MIP can effectively prevent the interference of impurity, which is the major problem of electrochemical detection.

Since the discovery of carbon nanotubes (CNTs) in 1991, they have been attracting great attention due to their prominent chemical, electrical and mechanical properties. A large number of studies have been established in various fields by using CNTs, such as energy storage, actuators and sensors[31,32]. Composite films of CNTs with other materials such as metal oxide, conducting polymers etc. are very attractive combinations of materials for the development of electrochemical sensors[33]. The electrodes modified with MIP/CNTs composites can show excellent electrocatalytic ability and high molecular recognition for some biological molecules due to their synergistic effect.

Herein, we developed molecularly imprinted electrochemical sensor (MIES) for detection of UA based on electrode modified with L-cysteine - functionalized multi-walled carbon nanotubes (Cys-MWCNTs), which possessed the features of large surface areas and acted as transducers to create a sensitive imprinting platform. After the optimization of the influential parameters such as pH of the electro-polymerized solution, scan cycles, washing time and rebinding time, the MIES showed high selectivity for the detection of the UA in serum samples.

Materials and Methods

Instruments

All electrochemical studies were performed with CHI660E electrochemical workstation (Chen Hua Instrument Company, Shanghai, China). A conventional three-electrode system was employed with a bare or modified electrode as working electrode, a saturated calomel electrode (SCE) as reference electrode and a platinum wire as the auxiliary electrode. pH measurements were carried out with a Hannah model pH meter.

Reagents

Uric acid, ascorbic acid, adenine, guanine, dopamine, potassium ferricyanide and o-phenylenediamine were purchased from Shanghai Chemical Reagent Co. Ltd, which are of analytical grade and without further purification. N-hydroxy succinimide (NHS) and 1-ethyl-(3-dimethylaminopropyl) carbamide hydrochloride (EDC) were purchased from Aladdin Reagent Company (China). Multi-walled carbon nanotubes (MWCNTs) were purchased from Nanjing Jicang Nanotechnology Co., Ltd (China). The water used in the experiment was ultrapure water.

Preparation of Cys-MWCNTs nanocomposites

MWCNTs were carboxylated according to the previous study with a minor modification[34]. Briefly, 50 mg of MWCNTs were dispersed into 40 mL mixture of H_2SO_4-HNO_3 (3:1 (v/v)) and stirred for 4 h. Upon diluting with 100 mL of ultrapure water, the black products were centrifuged, washed with ultrapure water several times until the filtrate was neutral, followed by drying in vacuum for 24 h. Then, 10.0 mg of the treated MWCNTs and 10.0 mg L-cysteine were dispersed in 10 mL of ultrapure water by ultrasonic agitation for 30 min to obtain a homogeneous MWCNTs suspension. Subsequently, EDC and NHS coupling agents were added into mixture and stirred for 24 h at room temperature. During this process, amide reaction between the carboxyl group on the MWCNTs and the amino group on the L-cysteine took place. The Cys-MWCNTs were obtained after mixture was centrifuged and rinsed with ultrapure water[35].

Preparation of Cys-MWCNTs modified electrode

Prior to modification, a glassy carbon electrode (GCE) was first polished with a 0.05 μm alumina slurry, and then sonicated with nitric acid (30%), ethanol and ultrapure water for a few minutes, successively. Subsequently, 6 μL of Cys-MWCNTs suspension (1.0 mg mL^{-1}) was dropped on the pre-treated GCE surface with a micro-syringe and dried under an infrared lamp. This electrode was denoted as Cys-MWCNTs-GCE, where Cys-MWCNTs exhibited improvement of the analytical performances due to the excellent dispersity and the increase in the electroactive area of the electrode.

The functional monomer, o-phenylenediamine was electropolymerized as previously reported[36]. The Cys-MWCNTs-GCE was dipped in 0.1 M phosphate buffer solution (PBS) of pH 6.5 containing 0.01 M o-phenylenediamine and 1.0 mM UA. Then electropolymerization was performed by cyclic voltammetry (CV), where 20 consecutive cycles were applied in a potential range of 0 to +0.8 V at 50 $mV \cdot s^{-1}$.

After being washed by ultrapure water to remove excess monomers and physically adsorbed molecules, the modified electrode was repeatedly immersed in anhydrous ethanol to remove the UA template and then air-dried overnight. Thus, a MIP-Cys – MWCNTs-GCE (MIES) was made. The whole process of electrode preparation is shown in Scheme 1. A non-imprinted electrode (NIP-Cys-MWCNTs-GCE) was also prepared following the same procedure with the absence of the template molecules.

General procedure for detction of UA

After MIES were immersed in PBS solutions of pH 5.0 containing different concentrations of UA to rebind the analyte for 9 min, the current response of the MIES was recorded using differential pulse voltammetry (DPV) with $K_3[Fe(CN)_6]$ as a redox probe. Prior to the next cycle, the MIES was immersed in anhydrous ethanol for 12 min to remove the previously residual UA from the polymeric network.

Results and Discussions

Optimization of preparation conditions for MIES

Electropolymerization of o-phenylenediamine on Cys-MWCNTs-GCE

Fig. 1 (inset) shows the cyclic voltammograms of electropolymerization of o-phenylenediamine on Cys-MWCNTs-GCE in the presence of UA template. As can be seen from the Fig. 1, the polymerization current reduces with scan cycles increasing due to the formation of a non-conductive poly(o-phenylenediamine) (POD) film at the Cys-MWCNTs-GCE electrode surface, which hinders the electron transfer during polymerization.

Herein, we define a ΔI value, which refers to the peak current value of MIES in $K_3[Fe(CN)_6]$ solution after elution minus the peak current value of the same electrode adsorbing UA. The performance of a MIES strictly depends on the thickness of the molecularly imprinted film, which change with CV scan cycles during the electropolymerization. Therefore, the thickness of film was adjusted by optimizing CV scan cycles. As depicted in Fig. 1, with the increase in scan cycles from 5 to 20, the value of ΔI becomes larger due to the increment of number of imprinted sites in the polymer film. However, the value of ΔI decreases after the scan cycles of 20 since the thicker polymer film could cause to the poorer conductivity. Moreover, the template molecules located at the center of the thicker membrane are difficult to elute

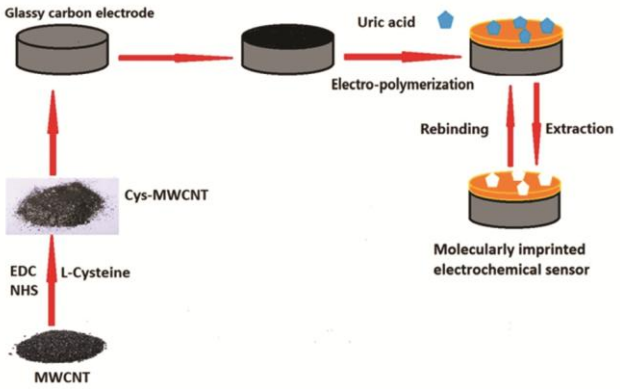

Scheme 1 — Procedure for the fabrication of the molecularly imprinted sensor for UA detection

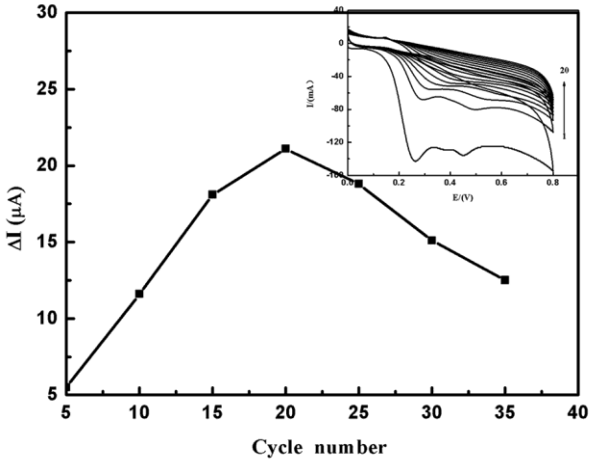

Fig. 1 — Effect of the cycle number on the peak current difference of the molecular imprinting sensor in $K_3Fe(CN)_6$ before and after elution. (inset) Cyclic voltammograms for the polymerization of o-phenylenediamine in the presence of UA (0.10 mM) in the PBS (pH=6.5) with a scan rate of 50mV·s^{-1}, scan cycle: 20

from the polymer, which is disadvantageous for the generation of imprinted sites. Therefore, the optimal scan cycles for electropolymerization MIP film were defined as 20.

Selection of polymerization solutions and pH value for the electropolymerization of MIP

The polymerization solutions for MIP, which are used during the electropolymerization, have an impact on the number of imprinted sites formed in polymer matrix, and consequently they may affect sensitivity of the sensor. For this reason, two MIP films were prepared using CV method with acetate buffer solution and PBS as polymerization solution, respectively. The results showed that the ΔI value of the MIP electrode prepared in PBS solution was significantly higher than that prepared in the acetate

buffer solution, so the PBS was selected as polymerization solution. Fig. 2 shows the value of ΔI of MIP-Cys-MWCNTs-GCE electrode prepared in PBS solution at different pH values. The experimental results show that the value of ΔI enhances with the increase of pH value when pH value is less than 6.5, and the value of ΔI reaches the maximum at pH 6.5. The reason may be that formation of possible hydrogen bonds between the POD film and UA. Amine groups of UA can form hydrogen bonds with the ketone groups of POD. In the same way, ketone groups of UA can also form hydrogen bonds with hydrogen atoms of benzene rings of the polymer[37]. The condition of pH=6.5 is most favourable for the formation of hydrogen bonds between UA and POD, which causes more imprinting cavities and a increase in the sensitivity of the sensor. On the contrary, on further rise in pH in PBS solution, the ability of formation of hydrogen bonds decline due to change of the structure of UA and POD, which reduce the number of effective imprinting cavities in polymer film. That is why the ΔI value decreases when the value of pH is above 6.5. Therefore, pH 6.5 was adopted as the optimum value of pH for the polymerization of imprinted film in the experiment.

Selection of eluent solution

The efficient removal of the template from the electropolymerized film is a significant detail to acquire selective electrochemical response in consequence of recognition cavities created by the extraction process. Therefore, the molecularly imprinted electrodes embedded UA molecules were immersed in acetone, anhydrous ethanol and 0.1 M NaOH solution for 12 min to remove analyte, respectively. The DPV responses of imprinted electrodes in $K_3[Fe(CN)_6]$ solution after removal of analyte were shown in Fig. 3. It can be seen that obvious oxidation peaks were observed after the molecularly imprinted electrodes were eluted with anhydrous ethanol and 0.1 M NaOH solution. Moreover, the peak current of the MIE eluted with anhydrous ethanol is larger than that eluted with 0.1 M NaOH solution. By comparison, the oxidation peak was small after eluted with acetone, indicating that it is difficult for acetone to elute the UA molecules embedded in the polymer film. The results showed that the elution effect of anhydrous ethanol was the best in the three eluent. Therefore, anhydrous ethanol was selected for the eluent.

Optimization of washing time

Washing time is one of the critical parameters for the formation of imprinted sites that affect the sensitivity of a MIES. The effect of the washing time on the peak currents of $K_3[Fe(CN)_6]$ was investigated by using DPV method after the MIP electrode embedded with UA molecules was dipped into in anhydrous ethanol at different time intervals. The curve of relationship between peak current and washing time was shown in Fig. 4. With increase of washing time, the peak current of $K_3[Fe(CN)_6]$ increases up to 12 min washing time. According to this result, it can be understood that the MIP electrode embedded with UA molecules hinders $K_3[Fe(CN)_6]$ probe from reaching the electrode surface, resulting in a decreasing peak current. With increase of washing time, the "cavities" left by the removal of UA

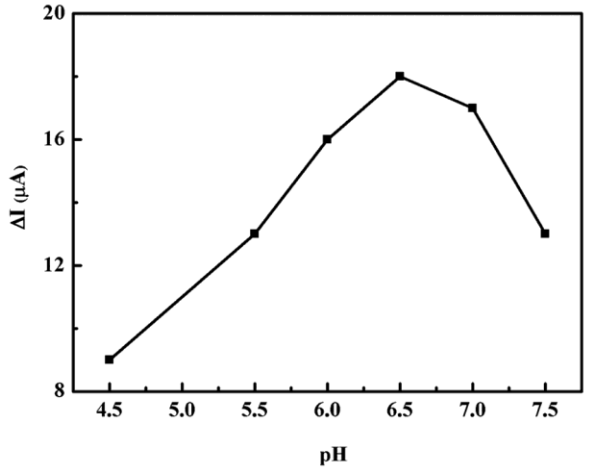

Fig. 2 — Effect of polymerization solutions pH on the peak current difference of the molecularly imprinted sensor in $K_3[Fe(CN)_6]$ solution before and after elution

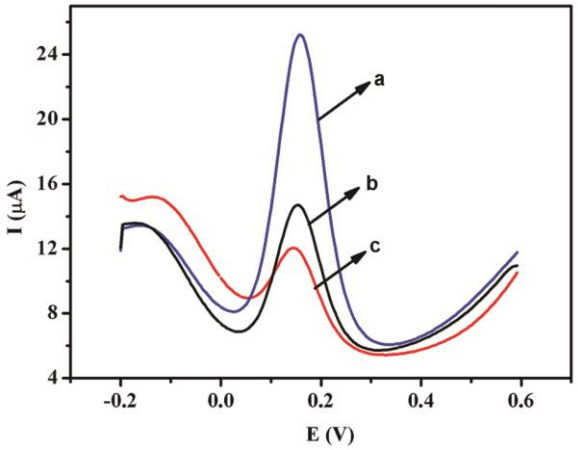

Fig. 3 — DPV curves of the molecularly imprinted electrodes in $K_3[Fe(CN)_6]$ solution after eluting with different eluents: (a) anhydrous ethanol, (b) 0.1 M NaOH, (c) acetone

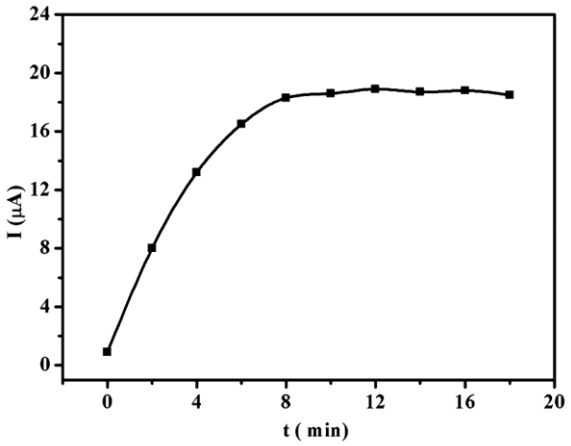

Fig. 4 — Effect of removal time on peak current of $K_3[Fe(CN)_6]$

gradually increased, and peak current increased due to more $K_3[Fe(CN)_6]$ reaching the electrode surface. When washing time reached 12 min, peak current remained almost constant owing to complete removal of UA molecules from electropolymerized film. Therefore, optimum washing time was performed as 12 min for the next studies.

Electrochemical characterization of the electrodes

The electrochemical characterization of MIP based sensor platform was carried out by using $K_3[Fe(CN)_6]$ redox probe. The cyclic voltammetry behaviour of different electrodes was shown in Fig. 5. As can be seen, the characteristic reversible electrochemical behaviour of $K_3[Fe(CN)_6]$ appears at the Cys-MWCNTs-GCE electrode and it shows high current response. In comparison, the current of $K_3[Fe(CN)_6]$ at the MIES is less than that of the Cys-MWCNTs-GCE, indicating that the rest part of the electrode surface is covered by the insulated POD membrane except for the imprinted caves left by the removal of UA. The NIP-Cys-MWCNTs-GCE, exhibits lower peak current in comparison to MIES in that the non-conductive polymer film deposited on the surface of electrode hinders the electron transfer between redox probe and the electrode surface.

The electrochemical impedance spectra of Cys-MWCNTs-GCE, MIES, and NIP-Cys-MWCNTs-GCE are shown in Fig. 6. The Nyquist plots of different electrodes represent at low frequency a straight line with a semi-circle at high frequency region. The semi-circle diameter corresponds to the electron transfer resistance (R_{et}), which controls the electron transfer kinetics of $K_3[Fe(CN)_6]$ at the electrode interface[38]. As can be seen, the NIP-Cys-MWCNTs-GCE displays a larger well defined semi-

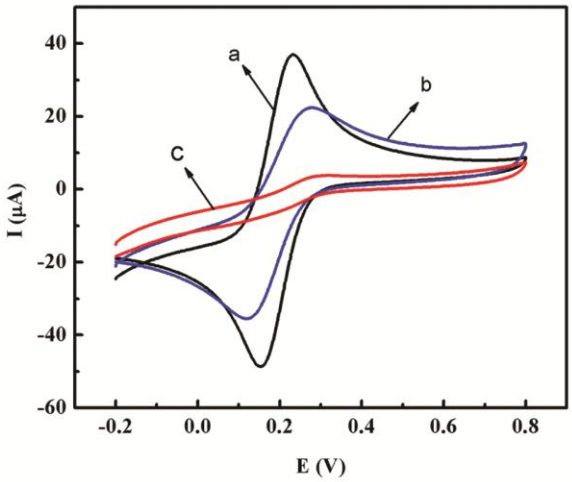

Fig. 5 — Cyclic voltammograms of (a) Cys-MWCNTs-GCE, (b) MIP-Cys-MWCNTs-GCE, (c) NIP-Cys-MWCNTs-GCE in 0.01 M $K_3[Fe(CN)_6]$ and 0.1 M KCl solution, scan rate: 50 $mV \cdot s^{-1}$

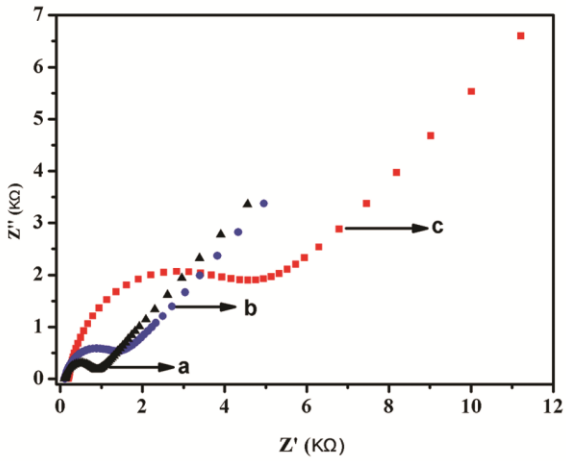

Fig. 6 — The electrochemical impedance spectra of Cys-MWCNTs-GCE (a), MIP- Cys-MWCNTs-GCE (b), NIP-Cys-MWCNTs-GCE(c) in 0.01 M $K_3[Fe(CN)_6]$ containing 0.1 M KCl

circle at high frequency region than the MIES, suggesting that it has larger electron transfer impedance, which results from the insulated polymer film covered the electrode surface. The R_{et} of MIES becomes smaller than that of NIP-Cys-MWCNTs-GCE in that a variety of template-shape imprinted sites are formed as channels making $K_3[Fe(CN)_6]$ probes tend to reach the surface of electrode. The Cys-MWCNTs-GCE demonstrates a low R_{et} value compared to the MIES, which means that the part surface of the Cys-MWCNTs-GCE is covered by the insulated polymer film except for the imprinted "cavities" left by the removal of the template molecule. According to the above result, it can be deduced that MIP film was obtained successfully.

Analytical performance of MIES

Selection of the pH value of solution

The influence of the pH value on the ΔI value between before and after rebinding UA was studied according to general procedure for the determination of UA. The experimental results showed that the ΔI value reached maximum in pH=5 PBS solution. This pH value favours the interaction between the polymer film and the template molecule by creating favourable conditions implying that above or below this value the template molecule or the polymer undergoes change in structure or functionality[39]. Therefore, the pH=5 PBS solution was used as the test solution.

Selection of rebinding time

The DPV responses of the MIES in $K_3[Fe(CN)_6]$ solution were investigated after the MIES was rebinding in PBS solution containing 2.0 μM UA for a certain time. It was found that the rebinding time had a distinct influence on the peak current and analytical sensitivity. As can be seen from the Fig. 7, the peak current gradually decreases with the increase in rebinding time. The peak current reaches its minimum at 9 min and remains constant thereafter, indicating that the adsorption equilibrium between the UA molecules and the imprinted cavities has been reached. During incubation, UA molecules re-enter the "cavities" matching their own structures with hydrogen bonds and cavity matching. The "cavities" in the imprinted membrane are reduced by the occupation of UA, resulting in the decrease of peak current. Thus, the period of 9 min was considered the ideal time for conducting the rebinding process in subsequent experiments.

A standard curve for UA

The DPV was performed for the determination of UA at the MIES in $K_3[Fe(CN)_6]$ solution after rebinding in different concentrations of UA for 9 min, and results was shown in Fig. 8a. As can be seen from figure with the increase of UA concentration, peak current decreases gradually. The peak currents of $K_3[Fe(CN)_6]$ have a good linear relationship with the concentration of UA in the range from 0.1 μM to 3.3 μM (Fig. 8b). The linear equation is I (μA) = 25.81-6.566 C (μM), with a correlation coefficient of 0.9989. The limit of detection is estimated to be 0.03 μM (S/N =3).

The comparison of the sensing performance of the MIES with those of some reported UA imprinted sensors is summarized in Table 1. The developed sensor based on the L-cysteine functionalized MWCNTs could provide a promising method for the sensitive detection of UA.

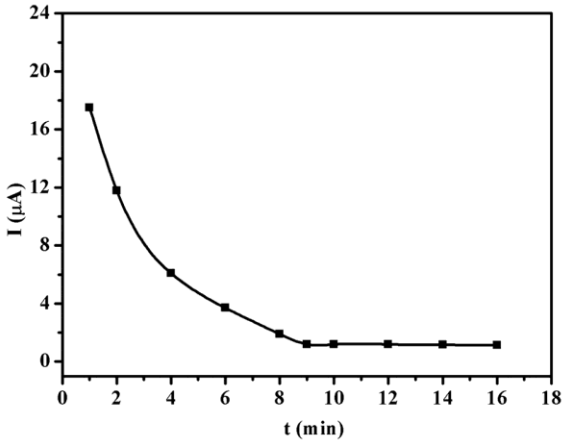

Fig. 7 — The effect of incubation time on peak current of $K_3[Fe(CN)_6]$

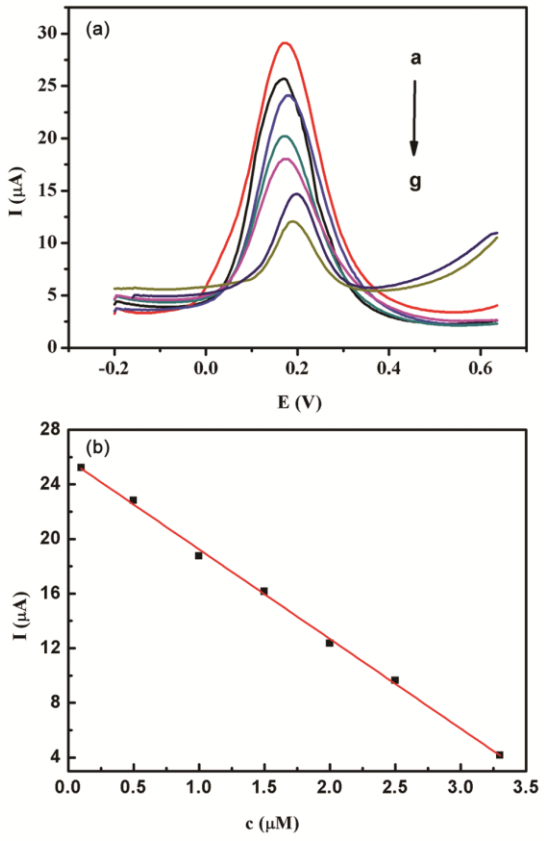

Fig. 8 — (a) DPV of MIES in 0.01 M $K_3[Fe(CN)_6]$ after rebinding in different concentrations of UA (from a to g, 0.1, 0.5, 1.0, 1.5, 2.0, 2.5, 3.3 μM) and (b) calibration curve of the peak current versus UA concentration

Selectivity of sensors

The molecular recognition capability of the MIES was investigated by employing UA structural

Table 1 — Comparison of the sensing performance of the MIES with those of some reported UA imprinted sensors

Sensor assembly	LOD	Linear range	Reference
MIP-sol-gel modified graphite	3:91 μg·mL^{-1}	4.78–106.96 μg·mL^{-1}	[41]
Fe_3O_4@C@MIT	0.02 μM	0.3–34 μM	[40]
indium–tin oxide	0.3 μM	0.15-1.15 mM	[37]
MWCNTs	22 μM	80-500 μM	[42]
Cys- MWCNTs	0.03 μM	0.1-3.3 μM	this work

Table 2 — Recovery results for serum sample

Samples	Measured (mM)	Added (mM)	Found (mM)	Recovery (%)	RSD (%, n = 3)
1	2.51	0.20	2.702	96.0	2.3
2	2.29	0.50	2.787	99.4	1.9
3	2.88	1.00	3.905	102.5	1.6

analogues adenine, guanine and ascorbic acid (AA), dopamine coexisting in serum as interfering substances, and their molecular structures were shown in Fig. 9. The selectivity was evaluated by calculating the ΔI value of the MIES in $K_3[Fe(CN)_6]$ solution between before and after rebinding in 2.0 μM UA and 10.0 μM interfering substances. As seen in Fig. 10, the ΔI value for AA and dopamine are about 0.3 μA (less than 2% of UA), even the concentrations of the interfering substances are 5 times that of UA, which adequately reveals that this MIES presents a superior selectivity towards UA. Compared with AA and dopamine, the ΔI value for adenine and guanine slightly increase (less than 10% of UA) for the molecular structures and size of adenine and guanine are similar to that of UA. The outstanding selectivity of the MIES can be mainly attributed to the recognition function of the large quantities of imprinted sites formed in MIP film. These imprinted sites can distinguish UA from other species through molecular size and functional group distribution, and rebind UA selectively by H-bonds interaction[40]. Thus, UA molecules are specifically accumulated on the MIES, whereas other coexistent molecules not complementary to the cavities interact with the sensor and mainly remained in the bulk solution.

Real samples analysis

The practical application of the MIES was evaluated by the analysis of the human serum real samples and the recovery study was carried out using standard addition method. The results of the recovery experiments were summarized in Table 2. As given in the Table 2, recovery values were found between 96.0% and 102.5%. Also, the calculated RSD values were found to be in range from 1.6% to 2.3% with high accuracy. These results proved that the proposed sensor could be successfully applied in real samples.

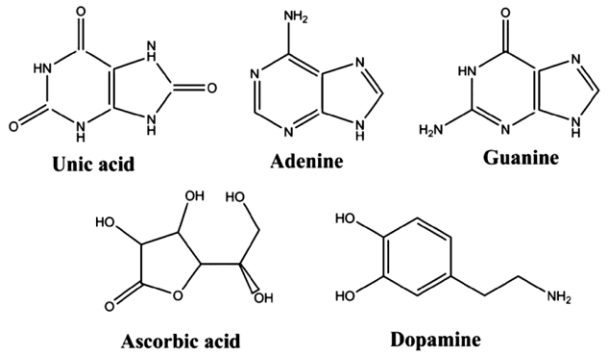

Fig. 9 — Molecular structures of uric acid and its structural analogues (adenine, guanine) and interfering substances coexisting in serum (ascorbic acid, dopamine)

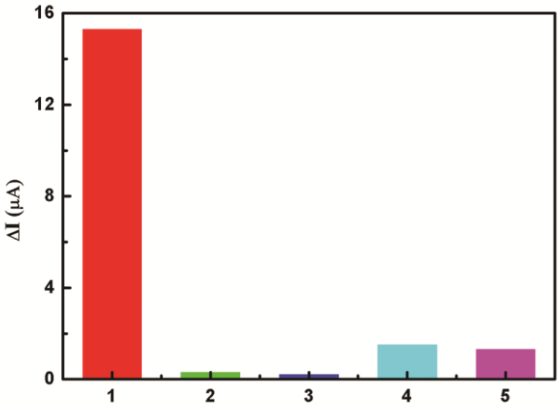

Fig. 10 — Comparison of the peak current difference on the MIES between before and after rebinding in 2.0 μM UA and 10.0 μM interfering substances: (1) UA, (2) AA, (3) dopamine, (4) adenine and (5) guanine

Conclusions

In this work, we developed a novel MIES based on the Cys-MWCNTs modified electrode, with o-phenylenediamine as the functional monomer and UA as the template molecule. The cyclic voltammetry and electrochemical impedance characterization confirmed the existence of the imprinted "cavities" in MIP film. The determination of UA was achieved by using DPV method with $K_3[Fe(CN)_6]$ as the probe molecules. Moreover, the MIES could be used for the estimation of UA in human serum in the presence of AA and dopamine as the major impurity. The results proved that MIES exhibited a superior selectivity and low detection limit (0.03 μM). The proposed biosensor showed a promising application in monitoring of biomolecules based on molecular imprinting technique.

References

1 Patel A K, Sharma P S & Prasad B B, *Mater Sci Eng C*, 9 (2009) 1545.
2 Azmi N E, Ramli N I, Abdullah J, Abdul-Hamid M A, Sidek H, Abd-Rahman S, Ariffin N & Yusof N A, *Biosens Bioelectron*, 67 (2015) 129.
3 Kong R M, Yang A, Wang Q, Wang Y, Ma L & Qu F, *Microchim Acta*, 185 (2018) 63.
4 Karami Z, Sohrabi N & Badoeidalfard A, *Biocatal Agric Biotechnol*, 24 (2020) 101549.
5 George S K, Dipu M T, Mehra U R, Singh P, Verma A K & Ramgaokar J S, *J Chromatogr B*, 832 (2006) 134.
6 Wijemanne N, Soysa P, Wijesundara S & Perera H, *Int J Anal Chem*, 2018 (2018) 1.
7 Hallaj T, Amjadi M & Mirbirang F, *Microchem J*, 156 (2020) 104841.
8 Sheng Y, Yang H, Wang Y, Han L, Zhao Y & Fan A, *Talanta*, 166 (2017) 268.
9 Amjadi M, Hallaj T & Nasirloo E, *Microchem J*, 154 (2020) 104642.
10 Badoei-dalfard A, Sohrabi N, Karami Z & Sargazi G, *Biosens Bioelectron*, 141 (2019) 111420.
11 Lu H, Li J, Zhang M, Wu D & Zhang Q, *Sens Actuators B*, 244 (2017) 77.
12 Krishnan R G, Rejithamol R & Saraswathyamma B, *Microchem J*, 155 (2020) 104745.
13 Guo X, Yue H, Song S, Huang S, Gao X, Chen H, Wu P, Zhang T & Wang Z, *Microchem J*, 154 (2020) 104527.
14 Pradhan S, Das R, Biswas S, Das D K, Bhar R, Bandyopadhyay R & Pramanik P, *Electrochim Acta*, 238 (2017) 185.
15 Zhao Q, Faraj Y, Liu L, Wang W, Xie R, Liu Z, Ju X, Wei J & Chu L, *Microchem J*, 158 (2020) 105185.
16 Jalalvand A R, *Sens Bio-Sens Res*, 28 (2020) 100330.
17 Baytak A K & Aslanoglu M, *Arab J Chem*, 13 (2020) 1702.
18 Noroozifar M, Motlagh M K, Akbari R & Parizi M B, *Biosens Bioelectron*, 28 (2011) 56.
19 Hussain M, Wackerlig J & Lieberzeit P A, *Biosens*, 3 (2013) 89.
20 Yüceba B B, Yaman Y T, Bolat G, Özgür E, Uzun L & Abaci S, *Sens Actuators B Chem*, 305 (2020) 127368.
21 Pan J, Chen W, Ma Y & Pan G, *Chem Soc Rev*, 47 (2018) 5574.
22 Chen W, Ma Y, Pan J, Meng Z, Pan G & Sellergren B, *Polymers*, 7 (2015) 1689.
23 Yang C, Ji X F, Cao W Q, Wang J, Zhang Q, Zhong T L & Wang Y, *Talanta*, 196 (2019) 402.
24 Lopes F, Pacheco J G, Rebelo P & Delerue-matos C, *Sens Actuators B*, 243 (2017) 745.
25 Liu B, Xiao B, Cui L& Wang M, *Mater Sci Eng C*, 55 (2015) 457.
26 Alizadeh T, Zare M, Reza M, Norouzi P & Tavana B, *Biosens Bioelectron*, 25 (2010) 1166.
27 He F, Jiang Y, Ren C, Dong G, Gan Y, Lee M J, Green R D & Xue X, *Solid State Ionics*, 297 (2016) 82.
28 Nezhadali A & Mojarrab M, *J Electroanal Chem*, 744 (2015) 85.
29 Pan Y, Shang L, Zhao F & Zeng B, *Electrochim Acta*, 151 (2015) 423.
30 Rezaei B, Boroujeni M K & Ensafi A A, *Sens Actuators B*, 222 (2016) 849.
31 Li L, Hu Z A, An N, Yang Y Y, Li Z M & Wu H Y, *J Phys Chem C*, 118 (2014) 22865.
32 Ansari S, *Trends Anal Chem*, 93 (2017) 134.
33 Balram D, Lian K Y, Sebastian N & Rasana N, *J Hazard Mater*, 406 (2021) 124792.
34 Pilehvar S, Rather J A, Dardenne F, Robbens J, Blust R & De W K, *Biosens Bioelectron*, 54 (2014) 78.
35 Wang W, Qiu Y, Zhang S, Li J, Lu X & Liu X, *Chin J Anal Chem*, 42 (2014) 835.
36 Cao W, Xiong H, Gao X, Zhang X & Wang S, *Anal Methods*, 6 (2014) 2349.
37 Chen P Y, Vittal R, Nien P C, Liou G S & Ho K C, *Talanta*, 80 (2010) 1145.
38 Wei Y, Kong L T, Yang R, Wang L, Liu J H & Huang X J, *Chem Commun*, 47 (2011) 5340.
39 Regasaa M B, Soreta T R, Femi O E, Ramamurthy P C & Subbiahraj S, *Sens Biosens Res*, 27 (2020) 100318.
40 Zhang C, Si S & Yang Z, *Biosens Bioelectron*, 65 (2015) 115.
41 Patel A K, Sharma P S & Prasad B B, *Mater Sci Eng C*, 29 (2009) 1545.
42 Chen P Y, Lin C Y & Ho K C, *AIP Conference Proceedings*, 1137 (2009) 284.